



**HAL**  
open science

## Enhanced differentiation of human induced pluripotent stem cells toward the midbrain dopaminergic neuron lineage through GLYPICAN -4 downregulation

Serena Corti, Remi Bonjean, Thomas Legier, Diane Rattier, Christophe Melon, Pascal Salin, Erik Toso, Michael Kyba, Lydia Kerkerian-le Goff, Flavio Maina, et al.

### ► To cite this version:

Serena Corti, Remi Bonjean, Thomas Legier, Diane Rattier, Christophe Melon, et al.. Enhanced differentiation of human induced pluripotent stem cells toward the midbrain dopaminergic neuron lineage through GLYPICAN -4 downregulation. *Stem Cells Translational Medicine*, 2021, 10 (5), pp.725-742. 10.1002/sctm.20-0177 . hal-03370622

**HAL Id: hal-03370622**

**<https://hal.science/hal-03370622>**

Submitted on 28 Oct 2021

**HAL** is a multi-disciplinary open access archive for the deposit and dissemination of scientific research documents, whether they are published or not. The documents may come from teaching and research institutions in France or abroad, or from public or private research centers.

L'archive ouverte pluridisciplinaire **HAL**, est destinée au dépôt et à la diffusion de documents scientifiques de niveau recherche, publiés ou non, émanant des établissements d'enseignement et de recherche français ou étrangers, des laboratoires publics ou privés.



Distributed under a Creative Commons Attribution - NonCommercial - NoDerivatives 4.0 International License

## PLURIPOTENT STEM CELLS

# Enhanced differentiation of human induced pluripotent stem cells toward the midbrain dopaminergic neuron lineage through GLYPICAN-4 downregulation

Serena Corti<sup>1</sup> | Remi Bonjean<sup>1</sup> | Thomas Legier<sup>1</sup> | Diane Rattier<sup>1</sup> |  
 Christophe Melon<sup>1</sup> | Pascal Salin<sup>1</sup> | Erik A. Toso<sup>2</sup> | Michael Kyba<sup>2</sup> |  
 Lydia Kerkerian-Le Goff<sup>1</sup> | Flavio Maina<sup>1</sup>  | Rosanna Dono<sup>1</sup> 

<sup>1</sup>Aix Marseille Univ, CNRS, Developmental Biology Institute of Marseille (IBDM), Turing Center for Living Systems, Parc Scientifique de Luminy, NeuroMarseille, Marseille, France

<sup>2</sup>Lillehei Heart Institute and Department of Pediatrics, University of Minnesota, Minneapolis, Minnesota

### Correspondence

Rosanna Dono, PhD, Aix Marseille Univ, CNRS, Developmental Biology Institute of Marseille (IBDM), Turing Center for Living Systems, Parc Scientifique de Luminy, Marseille, France.

Email: rosanna.dono@univ-amu.fr

### Funding information

National Institute of Arthritis and Musculoskeletal and Skin Diseases, Grant/Award Number: R01 AR075413; French Ministry of Higher Education, Innovation and Research Fellowship; BIOTRAIL PH.D. Program in Life Science, Marseille, France; Fondation pour la Recherche Médicale, Grant/Award Number: DEQ20141231766; Centre National de la Recherche Scientifique; Aix-Marseille University; Network of Centres of Excellence in Neurodegeneration (COEN) Pathfinder III, Grant/Award Number: COEN4014; Centre National de la Recherche Scientifique-Pre-Maturation Program; SATT Sud-Est "Technology Transfer accelerator"; Fondation de France, Grant/Award Number: 2013\_00043173; Association France Parkinson: 096038 and fellowship 4th year PH.D. thesis; Investissements d'Avenir, Grant/Award Numbers: ANR-17-EURE-0029, nEUro\*AMU; A\*MIDEX (Aix-Marseille Initiative of Excellence), Grant/Award Number: AMX-19-IET-004

### Abstract

Enhancing the differentiation potential of human induced pluripotent stem cells (hiPSC) into disease-relevant cell types is instrumental for their widespread application in medicine. Here, we show that hiPSCs downregulated for the signaling modulator GLYPICAN-4 (GPC4) acquire a new biological state characterized by increased hiPSC differentiation capabilities toward ventral midbrain dopaminergic (VMDA) neuron progenitors. This biological trait emerges both in vitro, upon exposing cells to VMDA neuronal differentiation signals, and in vivo, even when transplanting hiPSCs at the extreme conditions of floor-plate stage in rat brains. Moreover, it is compatible with the overall neuronal maturation process toward acquisition of substantia nigra neuron identity. HiPSCs with downregulated GPC4 also retain self-renewal and pluripotency in stemness conditions, in vitro, while losing tumorigenesis in vivo as assessed by flank xenografts. In conclusion, our results highlight GPC4 downregulation as a powerful approach to enhance generation of VMDA neurons. Outcomes may contribute to establish hiPSC lines suitable for translational applications.

### KEYWORDS

GLYPICAN-4, hiPSCs, hPSC-derived dopaminergic neurons, intrastriatal transplantation, self-renewal and differentiation

This is an open access article under the terms of the Creative Commons Attribution-NonCommercial-NoDerivs License, which permits use and distribution in any medium, provided the original work is properly cited, the use is non-commercial and no modifications or adaptations are made.

© 2021 The Authors. STEM CELLS TRANSLATIONAL MEDICINE published by Wiley Periodicals LLC on behalf of AlphaMed Press

## 1 | INTRODUCTION

The generation of ventral midbrain dopaminergic (VMDA) neurons is of prime interest for stem cell and medical research owing to the causal link between their death and Parkinson's disease (PD), the second most common neurodegenerative disorder.<sup>1</sup> During embryogenesis, VMDA neurons arise from the midbrain floor-plate and become organized into distinct subgroups characterized by different molecular, morphological and functional properties.<sup>2,3</sup> The largest VMDA neuron populations are found in two neighboring nuclei, the substantia nigra (SN) and the ventral tegmental area (VTA). The development and physiology of the SN neurons are extensively studied as their preferential and massive degeneration underlies the cardinal PD symptoms.<sup>1</sup> Distinctive features of SN neurons include extensive axonal projections<sup>4</sup> and particular sensitivity to cell death-triggering events compared with the other VMDA subtypes.<sup>5,6</sup>

Much of our understanding of SN VMDA neuron specification comes from research performed on primary cultures or tissues derived from rodent animal models. Recently, single cell transcriptome analysis of developing VM derived from human and mouse embryos revealed differences in developmental timing, proliferation rate and progenitor generation in human embryos, features likely critical for acquiring a proper VMDA subtype phenotype.<sup>7</sup> These and other discoveries have reinforced the importance of research on human models of VMDA neurons.

Human pluripotent stem cells (hPSCs) have emerged among the best human cellular sources of VMDA neurons *in vitro* to identify signals required for the acquisition of their neuronal identity and physiology. hPSC-derived SN VMDA neurons from PD patients and healthy donors have also been successfully exploited to uncover causalities of the selective vulnerability of SN neurons in PD and molecular events associated with their degeneration.<sup>8</sup> Furthermore, these cells have become a valuable experimental platform for drug discovery and PD personalized medicine.<sup>9-11</sup> *In vivo*, hPSC-derived VMDA neurons are considered potential therapeutics for PD treatment. Outcomes from preclinical studies showing that hPSCs-derived VMDA progenitors engrafted in the striatum of rat or monkey PD models survive, integrate into the host structure, and provide functional recovery<sup>12,13</sup> have now set the basis for the first clinical trials in PD patients.<sup>14,15</sup> *In view of these promising therapeutic perspectives for PD, intense research efforts are focused on defining strategies to optimize generation of authentic and functional VMDA neurons for in vitro and in vivo applications.*

The most recent and efficient differentiation protocols enabling generation of VMDA neurons from hPSCs rely on their stimulation with SHH, WNT and FGF, the three morphogenic signals controlling floor-plate induction with VM identity in embryos. To recapitulate the *in vivo* situation, these factors are added to the hPSC differentiation medium at precise concentrations and time points.<sup>12,13,16-19</sup> Despite good successes, extensive research is currently performed to identify the most

### Significance statement

Human pluripotent stem cells are a promising resource for disease modeling, drug discovery, and cell replacement therapy, given their potential to differentiate into all body cell types. The authors identify GLYPICAN-4 (GPC4) downregulation as a new and promising approach to promote more efficient generation of ventral midbrain dopaminergic neurons from human induced pluripotent stem cells (hiPSCs) both *in vitro* and after transplantation in rat brains. The reduced *in vivo* tumorigenesis of hiPSCs with downregulated GPC4 levels also points to greater safety of these ventral midbrain dopaminergic neurons in cell transplants.

suitable medium formulation for optimal generation of VMDA progenitors from hPSCs for *in vitro* and *in vivo* applications.

We explored an alternative approach for enhancing the differentiation propensity of human induced PSCs (hiPSCs) toward VMDA neurons, based on modulating expression levels of the cell membrane protein GLYPICAN-4 (GPC4). GPC4 is a member of the heparan sulfate proteoglycan family (HSPG) GLYPICANS, which are known to regulate developmental processes by fine-tuning cellular responses to instructive extracellular proteins.<sup>20-23</sup> Our strategy relies on the rationale that the three morphogens, SHH, WNT, and FGF, required for induction of a floor-plate with VM identity *in vivo* are modulated by GPC4. The possible influence of targeting GPC4 on hiPSC differentiation properties was supported by our previous studies on mESCs, showing that downregulating *Gpc4* confers to cells enhanced lineage entry properties under differentiation conditions, at the expense of self-renewal and tumorigenesis by modulating WNT signaling levels.<sup>24</sup> Furthermore, *Gpc4* mutant mESCs differentiated more efficiently than control cells into DA neurons, improving motor recovery upon brain transplantation in PD rat models.<sup>25</sup>

Here we identify downregulation of GPC4 as a new molecular setting enhancing the differentiation properties of hiPSCs toward the VMDA neuron lineage. By using the floor-plate based differentiation strategy, we show that hiPSCs with reduced GPC4 exhibit enhanced capability to acquire a SN VMDA progenitor fate *in vitro*, compatible with the overall neuronal maturation process into VMDA neuron with SN identity, while retaining self-renewal and pluripotency *in vitro* stemness conditions. *In vivo*, these cells show reduced tumorigenic potential in flank xenografts, and display enhanced propensity to generate VMDA progenitors when grafted as floor-plate cells in the DA denervated striatum of a PD rat model. Taken together, our results identify GPC4 as new cell intrinsic determinant controlling the acquisition of VMDA neuron fate by hiPSCs both *in vitro* and *in vivo*. The GPC4-downregulation strategy in hiPSCs can synergize with currently applied protocols to enable robust generation of clinically relevant SN VMDA neurons.

## 2 | MATERIALS AND METHODS

### 2.1 | Human iPSC culture and VMDA neuron differentiation

WT 029 hiPSCs<sup>26</sup> and AICS-0023 (Coriell Institute for Medical Research) were maintained on Matrigel (Corning BV 354277)-coated plates with in mTeSR1 medium (ref 85 850, Stemcell Technologies) and passaged weekly with Accumax (Millipore). To obtain stable clones of the 029 hiPSCs with GPC4 downregulation, 029 hiPSCs, at 50% to 60% confluence, were transduced with a lentivirus containing GPC4 targeting shRNA. Polybrene (1 µg/mL) was added to increase the efficiency of infection. On the next day, the medium was replaced and puromycin selection (1 µm/mL) was performed for 7 days. The same procedure was followed to obtain the control line, CTRLsh. After puromycin selection, single clones were screened by qRT-PCR to check for GPC4 expression levels. For generating pools of AICS-0023 hiPSCs these cells were transduced with lentiviral vectors encoding for two GPC4 targeting shRNA and for shCTRL. After 5 days of puromycin selection, GPC4 transcript levels were analyzed in the hiPSC pools. The list of all tested shRNAs targeting GPC4 is reported in Table S1. In vitro differentiation of hiPSCs into VMDA progenitors was performed with a modified version of the protocol of Nolbrant et al<sup>19</sup> described in details in Supplemental data.

### 2.2 | Rats for cell transplantation

Male Wistar Han IGS Rats [Cri:WI(Han)] were used as graft recipients (Charles River). All rats received a unilateral injection of 6-hydroxydopamine (6-OHDA) in the SN of the left hemisphere. For graft experiment, the host rats were transplanted at 4 weeks post-6-OHDA-lesion inwith 40.000 CTRLsh or GPC4sh cells at d5 of differentiation toward a VM fate.

### 2.3 | Cell counts and statistical analyses

All experiments were performed and analyzed with independent biological replicates. Dots in graphs indicate the numbers of independent biological replicates for experiments. Quantitative analyses of immunostaining were performed manually with the aid of FIJI image processing software,<sup>27</sup> and results were reported as mean of 4 to 8 different fields for each biological replicate. Statistical analyses were performed using the most adapted test for each study (Mann-Whitney, One and two way ANOVA and unpaired t test) using the GraphPad Prism version 8 software. Statistics were further reported as: ns = not significant, \* = *P* value <.05, \*\* = *P* value <.01, \*\*\* = *P* value <.001.

### 2.4 | Ethics

All procedures involving the use of animals were performed in accordance with the European Community Council Directive of September

22, 2010 on the protection of animals used for experimental purposes (2010/63/EU) and were carried out by authorized persons. The experimental protocols were in compliance with French law and institutional Ethical Committee guidelines for animal research and approved by the local Ethical Committee (CEEA n°14). The project authorization is registered under the number: APAFIS #8214-2016121417291352.v5 delivered by the “Ministère de l'Enseignement Supérieur, de la Recherche et de l'Innovation”.

## 3 | RESULTS

### 3.1 | HiPSCs with reduced GPC4 levels retain long-term self-renewal and pluripotency while acquiring reduced tumorigenesis

To assess the expression profile of GPC4 in undifferentiated hESCs and hiPSCs, we screened the StemMapper database.<sup>28</sup> Bioinformatics analysis of the expression data from 41 hESC and 27 hiPSC lines revealed a consistent presence of GPC4 transcripts in all cell lines expressing stemness markers such as NANOG and SOX2 (Figure 1A). We then used shRNA-mediated GPC4 targeting to efficiently and stably reduce GPC4 levels in hiPSCs in order to investigate for GPC4 functions. By performing studies in HEK cells and hiPSCs, we identified two shRNAs efficiently targeting GPC4, namely GPC4sh5 and GPC4sh4 (see Supplementary Method, Figure S1, Table S1). We transduced the hiPSC line 029<sup>26</sup> with lentiviruses encoding these selected shRNAs to generate stable clones from each targeting sequence. Among them, we selected GPC4sh5-c5 and GPC4sh5-c10 as representative clones carrying the GPC4sh5 sequence and GPC4sh4-c8 and GPC4sh4-c11 as representative clones carrying the GPC4sh4 sequence (see Supplementary Method, Figures 1 and S1). As a matched control, we generated and used a pool of stable clones derived from 029 hiPSCs transduced with the nonmammalian sequence GFP (CTRLsh). QRT-PCR analyses showed a level of GPC4 downregulation of ~50% in GPC4sh5-c5 and GPC4sh5-c10, and of ~80% in GPC4sh4-c8 and GPC4sh4-c11 compared with WT and CTRLsh hiPSCs (Figures 1B and S2A). GPC4 downregulation in these clones was confirmed by immunocytochemistry and western blots (Figures 1C, S1G-H, and S2 B).

We then assessed whether GPC4 downregulation affected hiPSC self-renewal and pluripotency. Under standard stemness conditions, GPC4sh hiPSCs stained for the pluripotent stem cell marker alkaline phosphatase (AP) as did control cells (Figure 1D). GPC4sh cells also showed growth and survival rates similar to control hiPSCs, as evidenced by the comparable cell cycle (Figures 1E and S2C), timing for confluence (Figures 1F and S2D), proliferation rate (phospho-Histone3 (pHH3) positive cells; Figures 1G S2E) and cell survival (cleaved-Caspase3; Figures 1G and S2E). Additionally, GPC4sh hiPSCs expressed levels of epiblast and pluripotency factors such as OTX2, OCT4, NANOG, and SOX2, comparable to controls as assessed at RNA (Figures 1H and S2F) and protein levels (Figures 1I,J and S2G,H). Collectively, these results show that

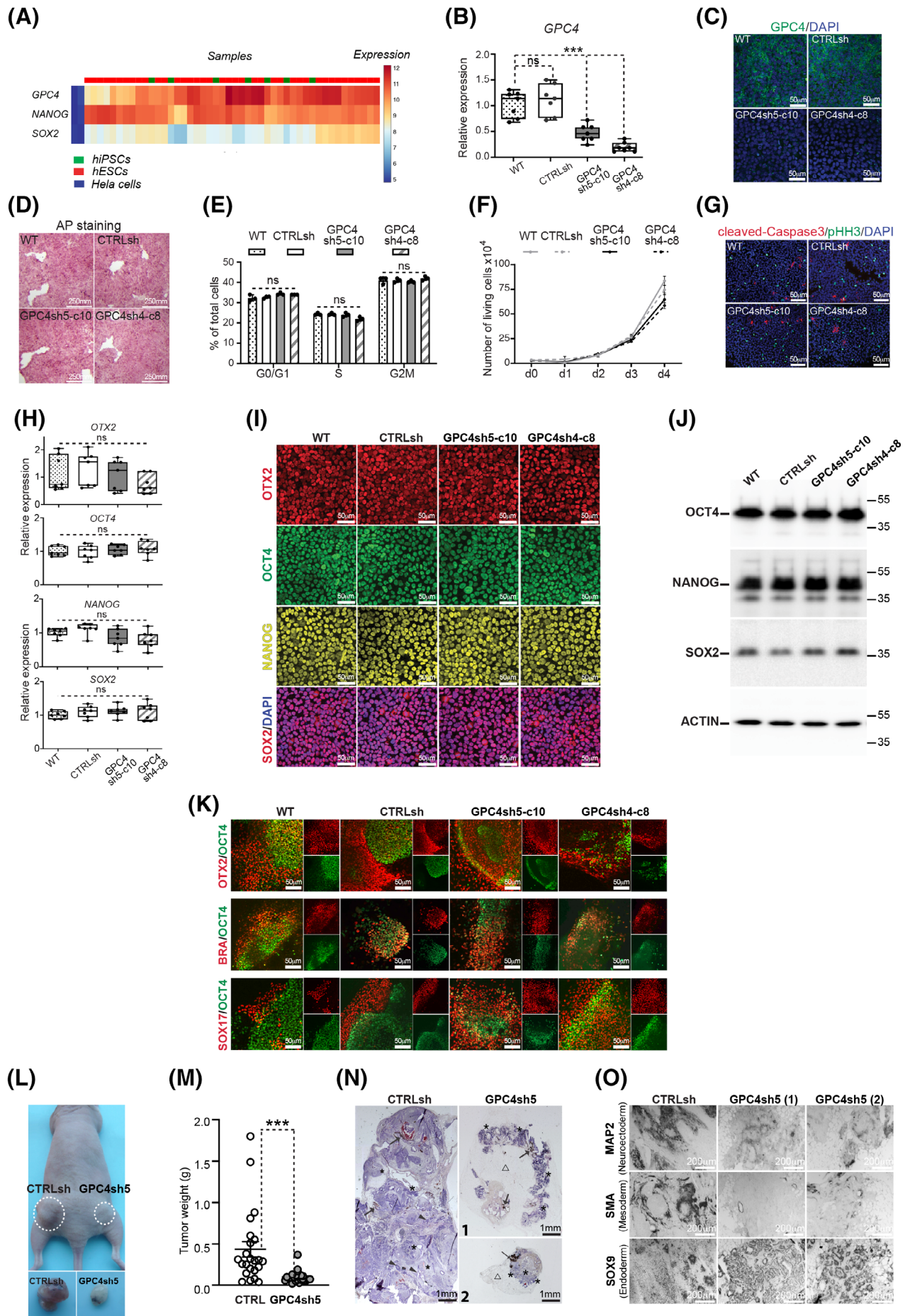


**FIGURE 1** Legend on next page.

GPC4 is dispensable for maintenance of hiPSC identity and self-renewal.

Next, we analyzed the pluripotent differentiation potential of GPC4sh hiPSCs in vitro and in vivo by performing embryoid body (EB)-mediated spontaneous differentiation and teratoma formation assays, respectively.<sup>29</sup> By using immunocytochemistry, we found that differentiating GPC4sh EBs exhibit loss of the hiPSC marker OCT4 and express markers of the three germ layers, such as OTX2 for Neuroectoderm, BRA for Mesoderm and SOX17 for Endoderm, similar to controls (Figures 1K and S2I). This indicates that GPC4sh hiPSCs retain pluripotency potential and lineage entry in EB-mediated spontaneous differentiation. Instead, assessment of developmental capacity by performing flank xenografts in nude mice revealed a ~4.5-fold reduced tumor formation in GPC4sh hiPSCs compared with controls (Figure 1L,M). Interestingly, histological and immunohistochemical analysis revealed that reduced GPC4 levels in hiPSCs not only reduce tumor formation in size but also affect the morphological feature of teratomas. In particular, derivatives of the three germ lines, endoderm, neuroectoderm and mesoderm, were found in CTRLsh hiPSCs as shown by the presence of SOX9-, MAP2-, and SMA-positive cells. Instead, GPC4sh hiPSCs generated predominantly endodermal derivatives. Therefore, loss-of-GPC4 impairs teratoma development (Figure 1N,O).

Altogether, these results show that GPC4 downregulation is compatible with maintenance of self-renewal and pluripotency in stemness conditions, whereas it impairs hiPSC tumorigenic potential following in vivo transplantation.

### 3.2 | Downregulation of GPC4 in hiPSCs promotes generation of VMDA progenitors in vitro

By re-analyzing expression of GPC4 in a previously published single-cell RNA-seq dataset from human embryo VM cells,<sup>7</sup> we found five distinct cell types sharing high probability of GPC4 expression: four radial glia-like (Rgl) cells (hRgl1, hRgl2a, hRgl2b, hRgl3) and one floor-plate progenitor [lateral floor-plate progenitors (hProgFPL)] (Figure S3A). Intriguingly, analysis of this RNA-seq dataset revealed drastic differences in the probability expression of the other GPC family members. In particular, we found lack of expression for GPC5 and GPC6, restricted expression of GPC3 to serotonergic neurons and of GPC2 to postmitotic DA progenitors (Figure S3B). Instead, GPC1 probability expression partially overlapped with GPC4 in hRgl2a and hRgl2b cells (Figure S3B). As Rgl cells within the human mesencephalon are neurogenic and serve as DA neuron progenitors,<sup>30</sup> the restricted localization of GPC4 transcripts to distinct precursors of VMDA neurons could underlie functional implications during early VMDA generation.

We examined the differentiation potential of GPC4sh hiPSCs toward VMDA neurons by applying the protocol of Nolbrant et al.<sup>19</sup> With this protocol, neuroepithelial cells generated via the dual SMAD inhibition approach are directed toward a floor-plate and then a VMDA progenitor identity by progressive activation of SHH, WNT and FGF8 signaling pathways. Afterwards, cells are exposed to factors promoting survival and terminal differentiation to generate functional VMDA neurons in vitro (Figure S3C). The differentiation profile of

**FIGURE 1** Characterization of WT, CTRLsh and GPC4sh hiPSC lines at the undifferentiated stage. A, Heatmap showing GPC4, NANOG, and SOX2 mRNA expression levels in 41 hESCs and 7 hiPSCs. The two cells lines on the left not expressing GPC4, NANOG, and SOX2 correspond to HELA cells. B, Graph reporting qRT-PCR analyses of GPC4 mRNA levels in WT, CTRLsh, GPC4sh5-c10, and GPC4sh4-c8 hiPSCs. Note reduced GPC4 levels in GPC4sh5-c10 and GPC4sh4-c8 vs WT and vs CTRLsh hiPSCs (GPC4sh5-c10:  $53 \pm 6\%$ ; GPC4sh4-c8:  $81 \pm 3\%$ ). Dots in each column indicate the number of independent biological replicates ( $n = 7$ ). The same representation is used for all graphs reported in this and following figures. Data are presented as mean  $\pm$  SEM. One-way ANOVA: \*\*\* $P < .001$ . C, Immunostaining analysis of GPC4 (green) and DAPI (blue) in the same hiPSCs lines. D, Alkaline phosphatase (AP) staining. E, Cell cycle analysis. Proportion of cells in G0/G1, S, and G2/M phases are shown as percentage ( $n = 3$  biological replicates). Data are reported as mean  $\pm$  SEM. One-way ANOVA: ns = not significant. F, Number of living cells at the indicated days of culture reported as total counts. Data are presented as mean  $\pm$  SEM ( $n = 3$  biological replicates). One-way ANOVA: ns = not significant. G, Immunofluorescence analysis of Cleaved Caspase 3 (red), phospho-Histone H3 (pHH3) (green) and DAPI (blue) shows no differences in cell survival nor mitosis between the hiPSCs lines. H-J, Molecular analysis of OTX2, OCT4, NANOG, and SOX2 expression by qRT-PCR analysis (H; Data are presented as mean  $\pm$  SEM of  $n = 7$  biological replicates. One-way ANOVA: ns = not significant), immunofluorescence (I) and western blot analyses of total protein extracts (J). Actin protein levels were used as loading controls in all western blots of these studies. K, Immunofluorescence analysis of EB-mediated spontaneous differentiation of WT, CTRLsh, GPC4sh5-c10, and GPC4sh4-c8 hiPSCs after 21-days of in vitro culture. Cells expressing OTX2, BRACHURY (BRA), and SOX17 correspond to cells undergoing ectoderm, mesoderm and endoderm lineage entry respectively. OCT4 staining was used to distinguish between undifferentiated hiPSCs (single OCT4 positives) and cell lineage-biased but not fully committed cells (double positive with OCT4). L, Teratoma assay: Top panel, representative image of mice carrying cell grafts after 9 weeks. Bottom panels, representative image of dissected tissues derived from injected controls and GPC4sh hiPSCs. M, Quantitative analysis of the weight of dissected tissue masses. Whereas control hiPSCs developed tumors of an average weight of  $0.435 \pm 0.093$  g, GPC4sh hiPSCs formed smaller tissue masses with an average weight of  $0.101 \pm 0.014$  g. Data are presented as mean  $\pm$  SEM from two independent experiments (CTRL, corresponding to WT+ CTRLsh tumors:  $n = 23$ ; GPC4sh:  $n = 24$ ). One-way ANOVA: \*\* $P < .001$ . See also Figures S1 and S2. N, Hematoxylin/eosin staining of paraffin sections from dissected tissues in (L). Teratoma-like structures are observed in samples derived from CTRLsh hiPSCs, as evidenced by the presence of the three germ layer derivatives (neuroectoderm; arrowheads; mesoderm: stars; endoderm: asterisks), but not in samples from GPC4sh hiPSCs in which more fibrillar-like structures (triangles right panels) as well as large patches of endodermal-like tissues (asterisks) are most apparent. Note the presence of pigmented cells possibly of neural crest origin in both CTRLsh and GPC4sh hiPSCs (arrows). O, Immunodetection of the markers MAP2 for neuroectoderm, SMA for mesoderm, and SOX9 for endoderm. Note that, in contrast to CTRLsh hiPSCs, GPC4sh hiPSCs generate predominantly endodermal derivatives, as shown by the presence of SOX9 positive cells and sporadic or absent MAP2 and SMA expressing cells

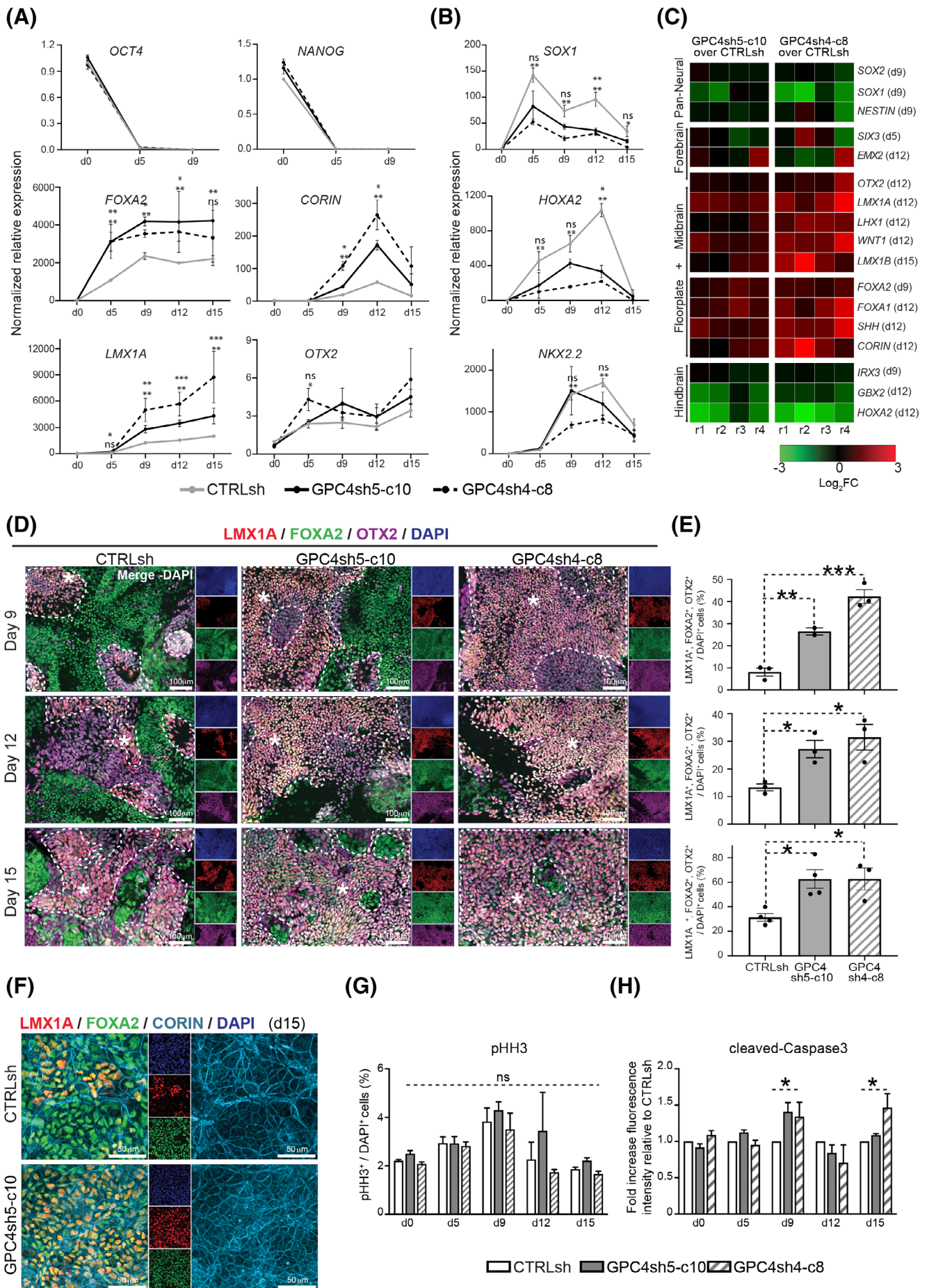


**FIGURE 2** Legend on next page.

CTRLsh and GPC4sh hiPSCs at the stage of midbrain floor-plate induction and VMDA progenitor generation [day 0 (d0) to d15] was assessed by following expression of well-established markers by qRT-PCR and immunocytochemistry (Tables S2 and S3).

In CTRLsh lines, the hiPSC markers *OCT4* and *NANOG* were drastically downregulated by d5 of differentiation and no more detectable by d9 (Figure 2A). This was accompanied by the upregulation of VMDA progenitor markers. In particular, *FOXA2* and *OTX2* expression levels peaked between d5 and d9 and were maintained at later differentiation stages (Figure 2A). *CORIN* expression peaked at d12 then was downregulated at d15. *LMX1A* transcripts were detected at later time points than those of *FOXA2* (d9 *LMX1A* vs d5 *FOXA2*; Figure 2A) and levels increased progressively (Figure 2A). The overall expression profile of markers during our differentiation studies was similar to that previously reported.<sup>12,16,19</sup> Interestingly, analysis of *GPC4* expression during VMDA neuron differentiation revealed a rapid decrease of transcripts levels from d0 to d5, suggesting that *GPC4* downregulation might be involved into the transition of hiPSCs from pluripotency to DA neuron lineage entry (Figure S3D).

In the four GPC4sh hiPSC cell clones, the kinetics of expression of these VMDA progenitor markers were similar to those seen in CTRLsh (Figure 2A), but significant differences in transcript levels were found at all time points analyzed, except for *OTX2*, whose expression level was similar to controls (Figures 2A and S3F). *FOXA2*, *CORIN*, and *LMX1A* transcripts were on average between 1.5-fold to 3-fold higher in GPC4sh cells (Figure 2A). In particular, *FOXA2* upregulation was evident from early days of differentiation (d5), whereas *LMX1A*, and *CORIN* mRNA significantly increased starting from d9 of VMDA patterning (Figures 2A and S3F).

The differentiation protocol we used was optimized to obtain VMDA identity. However, it is widely known that VM-patterned

cultures can contain other contaminating neural progenitors.<sup>19</sup> We assessed whether *GPC4* downregulation in hiPSCs would affect generation of other precursor types. We first analyzed the expression of *SOX1*, a pan-neural marker expressed in all neural precursors with the exception of VMDA progenitors,<sup>31</sup> as well as *HOXA2* and *NKX2.2*, which are expressed in serotonergic progenitors and other brain regions such as hindbrain and lateral midbrain.<sup>32</sup> QRT-PCR analysis revealed that these three markers were expressed in differentiating cultures at early time points, but their levels were markedly reduced in the four GPC4sh lines compared with CTRLsh cells (Figures 2B and S3G). Instead, the expression levels of *SOX2* and *NESTIN*, two additional pan-neural markers also expressed by VMDA neuron precursors, were similar in differentiating CTRLsh and GPC4sh cells (Figure 2C). Taken together, these results indicate that *GPC4* downregulation in hiPSCs favors the generation of VMDA neuron progenitors rather than triggering a general increase of neural differentiation. Yet, the increased VMDA precursors might occur at the expenses of other neuronal cell types.

The preferential midbrain and floor-plate patterning of GPC4sh cultures was also corroborated by qRT-PCR analysis of genes commonly used to monitor the presence of contaminating forebrain and hindbrain cell populations. When compared with CTRLsh, GPC4sh cells showed increased transcript levels for genes activated in the midbrain and floor-plate (*OTX2*, *LMX1A*, *LMX1B*, *LHX1*, *WNT1*, *FOXA1*, *FOXA2*, *SHH*, *CORIN*), but decreased levels of those expressed in forebrain (*SIX3*, *EMX2*) and hindbrain (*IRX3*, *GBX2*, *HOXA2*), whose transcript levels were significant only at early differentiation stages (Figure 2C).

We further examined neural differentiation by performing immunofluorescence labeling of *NESTIN* and of differentiation of VMDA progenitors by performing triple immunofluorescence labeling of

**FIGURE 2** Downregulation of *GPC4* in hiPSCs promotes efficient generation of VMDA progenitors in vitro. A, Graphs reporting qRT-PCR analyses at the indicated time points of the pluripotency markers *OCT4* and *NANOG* (top) and of VMDA progenitor markers, *FOXA2*, *CORIN*, *LMX1A*, *OTX2* (middle and bottom) during in vitro VMDA differentiation of CTRLsh, GPC4sh5-c10, and GPC4sh4-c8 hiPSCs. B, Graphs reporting qRT-PCR analyses at the indicated time points of the pan-NSC marker (*SOX1*), not expressed in VMDA progenitors, and of genes expressed in other brain areas (*HOXA2*, *NKX2.2*) during in vitro VMDA differentiation of the same hiPSCs. Values from different experiments were normalized as described in Materials and Methods to take into account variations in the differentiation efficiency of each individual experiment (n = 3-6 biological replicates). Data are presented as mean ± SEM. Mann-Whitney: ns = not significant, P values reported, \*P < .05, \*\*P < .01, \*\*\*P < .001. Statistical analysis was performed comparing GPC4sh5-c10 and GPC4sh4-c8 vs the CTRLsh cells. C, Heatmap illustrating qRT-PCR analysis of pan-NSC markers (*SOX1*, *SOX2*, *NESTIN*), forebrain markers (*SIX3*, *EMX2*), and genes expressed in midbrain (*OTX2*, *LMX1A*, *LMX1B*, *LHX1*, and *WNT1*), floor-plate (*FOXA1*, *FOXA2*, *SHH*, *CORIN*), and hindbrain (*IRX3*, *GBX2*, *HOXA2*). Differential mRNA expression (Log<sub>2</sub>FC) in CTRLsh vs GPC4sh5-c10 (left panel) and GPC4sh4-c8 (right panel) are reported according to the shown scale (bottom). Each marker is shown at the peak of its expression (from d0 to d15; n = 4). D, Immunofluorescence analysis of *LMX1A* (red), *FOXA2* (green), *OTX2* (purple), and DAPI (blue) positive cells in CTRLsh, GPC4sh5-c10, and GPC4sh4-c8 cultures at the indicated time points of VMDA differentiation. *LMX1A*<sup>+</sup>, *FOXA2*<sup>+</sup>, *OTX2*<sup>+</sup> cells, which correspond to bona fide VMDA progenitors, are highlighted by dashed areas with a star. E, Quantification of the percentage of *LMX1A*<sup>+</sup>, *FOXA2*<sup>+</sup>, *OTX2*<sup>+</sup> VMDA progenitors over DAPI<sup>+</sup> (VMDA progenitors at d9: CTRLsh: 8.1 ± 1.8%; GPC4sh5-c10: 26.5 ± 1.6%; GPC4sh4-c8: 42.3 ± 3.1%; at d12: CTRLsh: 13.3 ± 1.2%; GPC4sh5-c10: 27.1 ± 3.1%; GPC4sh4-c8: 31.4 ± 4.6%; at d15: CTRLsh: 31.4 ± 3.1%; GPC4sh5-c10: 62.7 ± 7.6%; GPC4sh4-c8: 62.7 ± 9.0%). Data are presented as mean ± SEM (n = 2-3 biological replicates). One-way ANOVA: \*P < .05, \*\*P < .01, \*\*\*P < .001. F, Immunofluorescence analysis of *LMX1A* (red), *FOXA2* (green), *CORIN* (light blue) and DAPI (blue) positive cells in CTRLsh and GPC4sh5-c10 lines at d15 of VMDA differentiation. G and H, Graphs reporting the percentage of phospho-Histone H3 (pHH3)<sup>+</sup> over DAPI<sup>+</sup> cells (G) and the quantification of the mean fluorescent intensity of cleaved-Caspase3 (H) in CTRLsh, GPC4sh5-c10, and GPC4sh4-c8 cultures at the indicated time point of VMDA neuron differentiation. A slight increase of cell death was observed in GPC4sh5-10 at d9, and in GPC4sh4-c8 at d9 and d15, possibly linked to a premature requirement of neurotrophic factors. Data are presented as mean ± SEM (n = 3). One-way ANOVA: \*P < .05. See also Figures S1, S4, S5 and S6

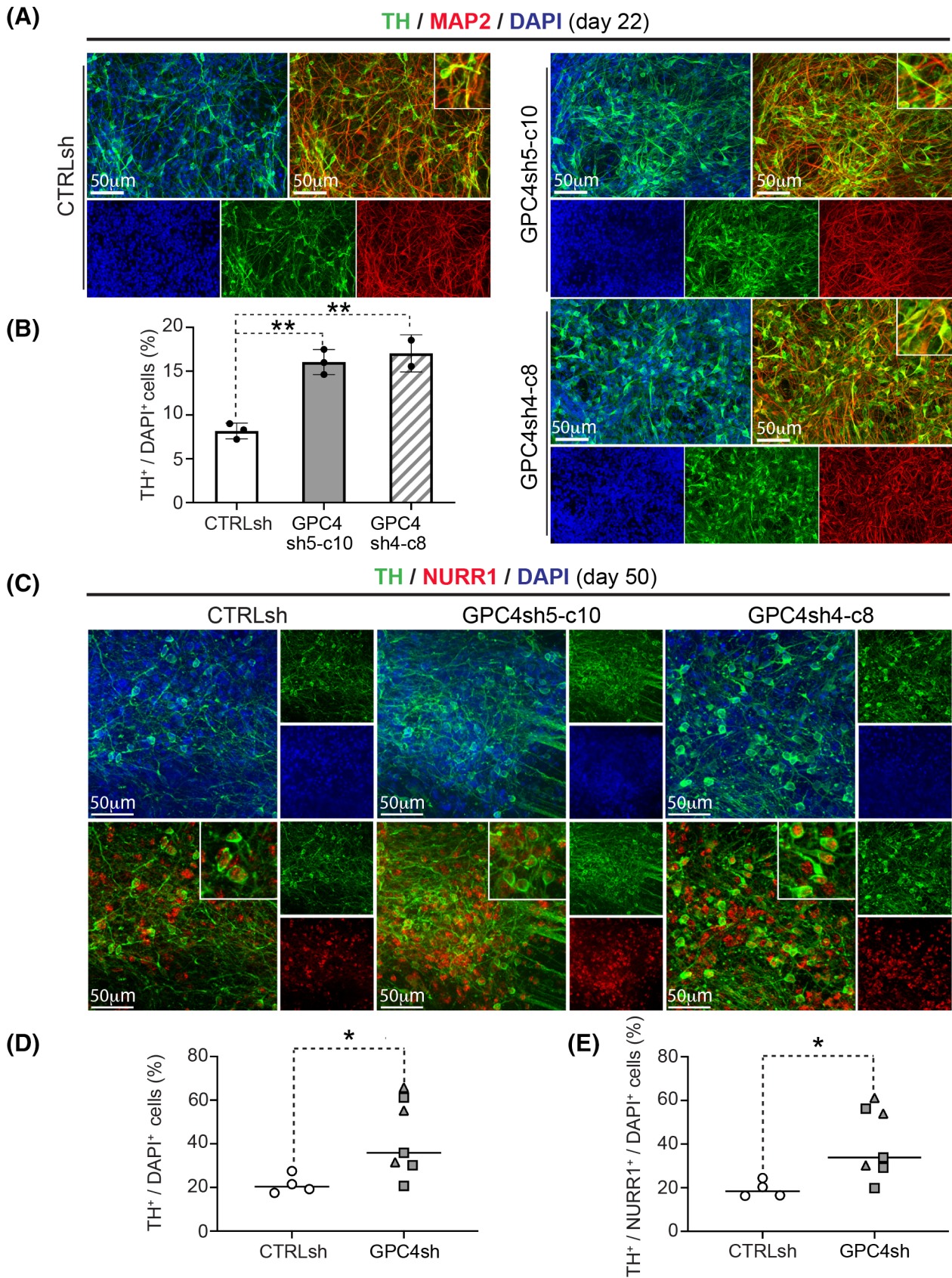


**FIGURE 3** Legend on next page.

LMX1A, FOXA2, and OTX2.<sup>33</sup> NESTIN staining showed that most CTRLsh and GPC4sh cells acquired a neural phenotype already by d9 (Figure S4A). Triple positive LMX1A, FOXA2 and OTX2 neural progenitors were found in both CTRLsh and GPC4sh, in increasing numbers between d9 and d15. But their proportion appeared markedly higher in cultures of all four GPC4sh lines, strengthening enhanced differentiation propensity toward VMDA precursors (Figures 2D,E and S4B). Quantitative analysis showed that the percentage of triple positive cells in GPC4sh cultures was ~3-fold to 6-fold higher than in CTRLsh lines at d9 (CTRLsh:  $8.1 \pm 1.8\%$ ; GPC4sh5-c10:  $26.5 \pm 1.6\%$ ; GPC4sh4-c8:  $42.3 \pm 3.1\%$ ) and remained at least ~2-fold higher at 12 and 15 days (eg, d15, CTRLsh:  $31.4 \pm 3.1\%$ ; GPC4sh5-c10:  $62.7 \pm 7.6\%$ , GPC4sh4-c8:  $62.7 \pm 9.0\%$ ; Figure 2E).

We further quantified the expression of individual markers by cells overtime. Concerning FOXA2 and OTX2, GPC4sh and CTRLsh cultures showed significant differences in the percentage of cells positive for these markers only at d9, whereas the percentage of cells positive for LMX1A were significantly higher at all time point analyzed (Figure S6). It is tempting to speculate that GPC4sh cells might have a higher competence for LMX1A expression compared with controls. Finally, we observed at day 15 enhanced proportion of cells expressing the floor-plate marker CORIN in GPC4sh cultures, as illustrated for GPC4sh5-c10, further pointing to their VMDA progenitor nature (Figure 2F). Therefore, independently on the VMDA marker used, GPC4sh hiPSCs outnumbered CTRLsh, indicating that GPC4 downregulation enhances the capability of hiPSCs to generate VMDA progenitors.

To assess the effect of GPC4 downregulation in a different hiPSC line, we examined the generation of VMDA precursors in the AICS-0023 hiPSCs targeted with CTRLsh and GPC4sh (Figure S5). Qualitative and quantitative analyses of cell pools showed a significant ~2 and ~1.8-fold increase into the percentage of VMDA precursors triple positive cells in GPC4sh cultures at d9 and d15 of differentiation respectively (d9:  $12.53 \pm 1.0\%$ ; GPC4sh:  $23.8 \pm 1.7\%$ . d15: CTRLsh:  $38.1 \pm 2.7\%$ ; GPC4sh:  $65.9 \pm 0.9\%$ ; Figure S5C and S5D). These results show that efficient differentiation of hiPSCs into VMDA precursors following GPC4 downregulation is not limited to one hiPSC line.

We next investigated whether the enhanced VMDA progenitor formation associated with GPC4 downregulation could be linked to changes in cell proliferation or survival. We performed immunocytochemical detection of dividing cells using the mitotic marker pHH3

and of apoptotic cells expressing active Caspase-3 at different time points (d0, d5, d9, d12, d15) of VMDA neuron differentiation. Qualitative and quantitative analyses did not reveal significant differences in either cell proliferation or survival between all four GPC4sh and CTRLsh cultures (Figures 2G,H and S4C).

Taken together, these results establish a specific role of GPC4 in fate decision during generation of VMDA precursors in hiPSCs. Its downregulation confers to hiPSCs a higher propensity for generation of VMDA progenitors, possibly at expense of other neural cell types, without changes of proliferation or survival of differentiating cells.

### 3.3 | VMDA neuron progenitors with downregulated GPC4 acquire a mature phenotype and a SN VMDA neuron identity

To explore whether the strategy of GPC4 downregulation in hiPSCs can promote terminal differentiation into functionally mature VMDA neurons, we first analyzed the expression of the DA synthesizing enzyme tyrosine hydroxylase (TH). In all clones of the 029 cell lines examined, numerous TH+ cells were visualized at d22, with co-expression of the pan neural marker MAP2 establishing their neuronal nature (Figure 3A). Interestingly, the number of cells expressing TH in GPC4sh differentiating cultures was ~2-fold enhanced compared with CTRLsh cells at d22 of differentiation (CTRLsh:  $8.8 \pm 0.5\%$ ; GPC4sh5-c10:  $16.0 \pm 0.8\%$ ; GPC4sh4-c8:  $17.2 \pm 1.6\%$ ; Figures 3A,B and S7A), d26 (Figures S7B and S7C) and d50 of DA neuron differentiation (Figure 3C,D). Of note, microscopic examination of AICS-0023 hiPSCs also revealed that the proportion of cells expressing TH in GPC4sh differentiating culture at d20 was ~1.7-fold higher than in controls (TH at d20: CTRLsh:  $13.6 \pm 4.0\%$ ; GPC4sh:  $21.6 \pm 4.0\%$ ; Figure S7D and S7E).

As cell types other than DA neurons express TH,<sup>34</sup> we tested whether TH+ cells also express NURR1, a protein crucial for progressive acquisition of a VMDA neuron neurotransmitter phenotype.<sup>33,35</sup> Cells in both CTRLsh and GPC4sh cultures were in great majority double positive for TH+/NURR1+ (Figure 3C,E), and can be thus considered as “bona fide” VMDA neurons.

We next analyzed the expression of other markers of functionally mature VMDA neurons. Remarkably, we found co-expression of TH with VMAT2 (involved in dopamine storage into vesicles and release;

**FIGURE 3** Downregulation of GPC4 in hiPSCs leads to an increased proportion of functionally mature DA neurons in vitro. A, Immunofluorescence visualization of TH (green), MAP2 (red) and DAPI (blue) expressing cells in CTRLsh, GPC4sh5-c10 and GPC4sh4-c8 cultures at d22 of VMDA differentiation. B, Graph reporting quantification of the percentage of TH+ neurons over DAPI+ cells in these cultures at d22 of VMDA differentiation. Note that GPC4sh lines exhibit significantly higher proportion of TH expressing neurons. Data are presented as mean  $\pm$  SEM of  $n = 2-3$  biological replicates. One-way ANOVA:  $**P < .01$ . C, Immunofluorescence staining of double TH+ (green) and NURR1+ (red) or DAPI (blue) positive neurons in CTRLsh, GPC4sh5-c10 and GPC4sh4-c8 cultures at d50 of VMDA differentiation. D and E, Graphs reporting quantification of the percentage of TH+ neurons over DAPI+ cells (D) and double TH+, NURR1+ neurons over DAPI+ cells (E) in these cultures at d50 of VMDA neuron differentiation (TH+ cells at d50: CTRLsh:  $22.7 \pm 2.5\%$  GPC4sh lines:  $44.4 \pm 6.1\%$ ). Square and triangle symbols in graphs correspond to values calculated for GPC4sh5-c10 and GPC4sh4-c8 cells, respectively. Note that most TH+ neurons in both CTRLsh and GPC4sh cultures were VMDA neurons as they are double positive for TH+/NURR1+ (CTRLsh:  $20.3 \pm 2.3\%$ ; GPC4sh lines:  $44.1 \pm 5.9\%$ ). Data are presented as mean  $\pm$  SEM ( $n = 2$  biological replicates). One-way ANOVA:  $**P < .01$ ,  $***P < .001$ . See also Figure S7

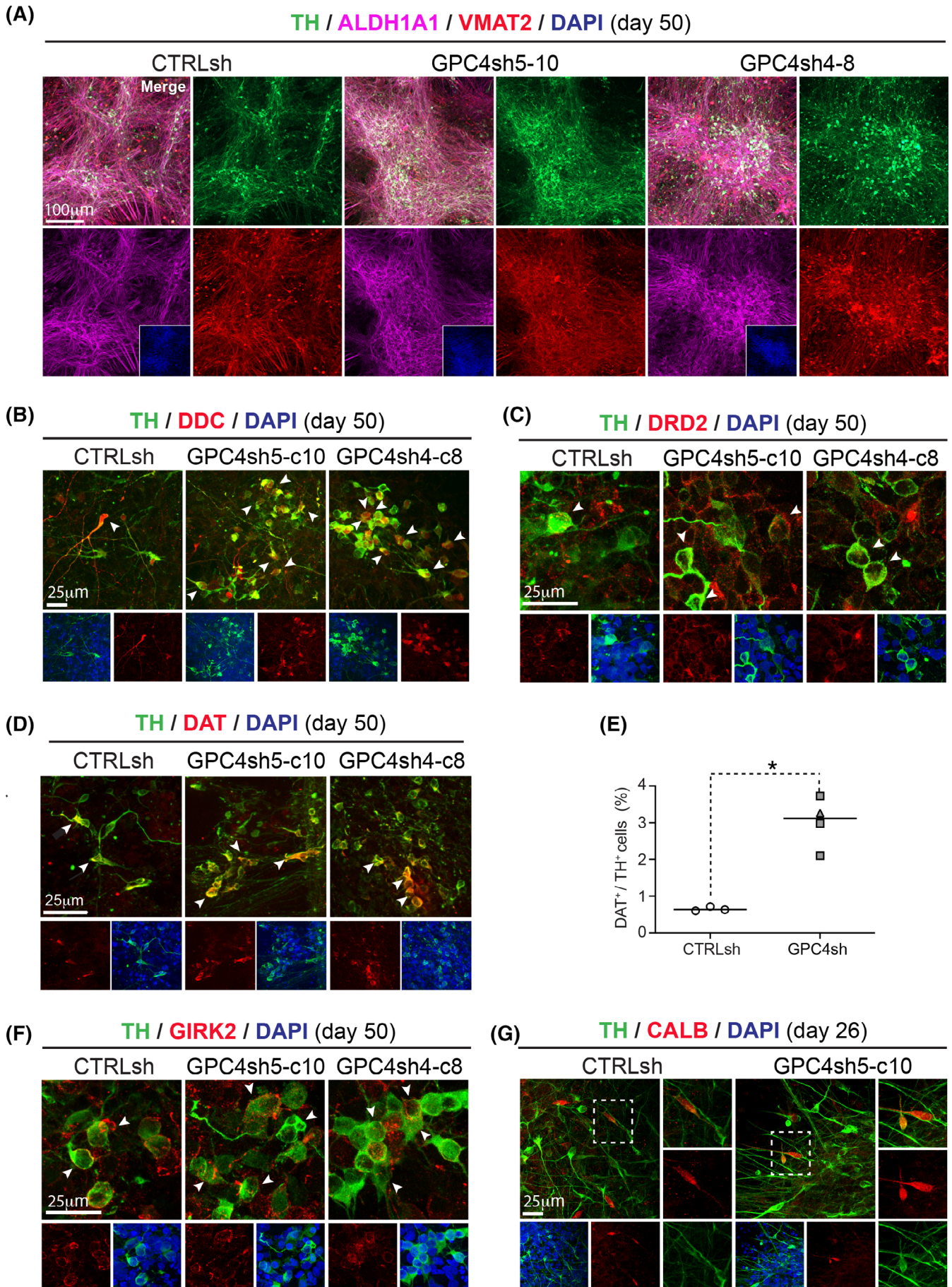


**FIGURE 4** Legend on next page.

Figure 4A), DDC (involved in dopamine production; Figure 4B) and DRD2 (dopamine receptor subtype expressed as autoreceptor in dopamine neurons; Figure 4C). Part of TH<sup>+</sup> neurons also co-expressed the membrane dopamine transporter DAT, which is one of the latest markers to be expressed during VMDA differentiation, in both CTRLsh and GPC4sh lines at d50 (Figure 4D). Quantitative analysis showed that their percentage was also higher in differentiating GPC4sh vs CTRLsh lines, consistent with their enhanced VMDA neuron differentiation properties (Figure 4E).

Interestingly, these differentiating cultures are enriched in TH neurons co-expressing ALDH1A1 (protecting neurons from the accumulation of dopamine aldehyde intermediates; Figure 4A) and GIRK2 (Figure 4F), whereas they contain only sporadic calbindin-positive TH neurons (Figure 4G). Of note, ALDH1A1 and GIRK2 are predominantly expressed in SN in contrast to calbindin, which is also highly expressed in the VTA.<sup>33,36</sup> Thus, these analyses revealed that the enhanced differentiation properties of GPC4sh cells observed at neuronal progenitor stage are preserved during all the differentiation process up to terminal differentiation into mature neurons with SN VMDA neuron identity.

### 3.4 | GPC4 downregulation in hiPSCs does not increase the presence of contaminant GABAergic, serotonergic, and glutamatergic neurons in VMDA cultures

Detailed knowledge about the neuronal subpopulations present in hiPSC derivatives is essential for their successful use in cell replacement therapy of PD. For example, the presence of contaminating serotonergic neurons appears to cause severe side effects such as dyskinesia.<sup>37</sup> We therefore analyzed transcript levels of key molecular markers of other neuronal populations often found in differentiating cultures, such as GABAergic, serotonergic and glutamatergic neurons. QRT-PCR analyses of GABAergic markers *GAD1* and *GAD2* at d29 and d35 showed no changes in transcript levels between CTRLsh and GPC4sh differentiating cells (Figure 5A). The serotonergic markers *5-HT*, *5-HTT* and *TPH2* were either not expressed at d29 and d35 of DA differentiation (for *5-HT* and *5-HTT*; data not shown) or showed no significant change (for *TPH2*) between

CTRLsh and GPC4sh cultures (Figure 5A). Similarly, glutamatergic marker genes, *vGLUT1*, *vGLUT2* and *GLS* were found predominantly unchanged at these time points (Figure 5A). To strengthen these data, we also investigated GABAergic and serotonergic markers by immunocytochemistry. CTRLsh or GPC4sh cells contained very few GABA<sup>+</sup> and 5-HT<sup>+</sup> neurons (Figure 5B,C). Regarding glutamatergic neurons, the different antibodies tested for vGLUTs did not provide good quality immunostainings. Overall, these results indicate that GPC4 downregulation in hiPSCs leads to a specific increase of VMDA neurons.

### 3.5 | Downregulation of GPC4 promotes specification of hiPSCs transplanted into rat brains at floor-plate stage toward VMDA progenitors

To establish whether GPC4sh hiPSCs are competent to acquire a VMDA progenitor fate in vivo, we performed cell transplantation experiments in rat brains. Currently, transplantation experiments with hESC and hiPSC derivatives make use of cell differentiated in vitro for 16- to 25-days in order to well establish the VMDA neuron identity and to enrich cultures with postmitotic progenitors.<sup>12,13,16,38</sup> We have previously reported that GPC4sh mESCs efficiently generate functional VMDA neurons even though they were transplanted after only 4-days of in vitro spontaneous differentiation.<sup>25</sup> We therefore assessed the differentiation properties of GPC4sh hiPSCs in vivo by transplanting them at floor-plate stage after a short pulse of SHH and WNT agonist (Figure 6A). Specifically, cells were differentiated in vitro for 5 days, a time point in which differentiating cells display floor-plate features and the efficient differentiation properties of GPC4sh cells become apparent (Figure 2A).

We grafted 40 000 cells, either CTRLsh-derivatives or GPC4sh-derivatives, into the striatum of adult rats with prior 6-hydroxydopamine-induced lesion of the nigrostriatal DA neurons (Figure 6A). Analyses were performed 9 weeks after transplantation. Despite differences in their size, which was ~3-fold higher for CTRLsh vs GPC4sh (CTRLsh:  $0.9 \pm 0.2 \text{ mm}^3$ , GPC4sh:  $0.3 \pm 0.1 \text{ mm}^3$ ; Figure 6B-D), both CTRLsh and GPC4sh grafts did not show signs of aberrant features such as tumor formation or necrosis, indicating a healthy state of transplanted cells.

**FIGURE 4** VMDA neuron progenitors with downregulated GPC4 acquire a mature phenotype and a SN VMDA neuron identity. A-E, Immunostaining showing the co-expression of (A) TH (green), ALDH1A1 (purple), VMAT2 (red) and DAPI (blue), (B) TH (green), DDC (red), and DAPI (blue), (C) TH (green), DRD2 (red), and DAPI (blue), (D) TH (green), DAT (red) and DAPI (blue) in CTRLsh, GPC4sh5-c10 and GPC4sh4-c8 cultures at d50 of VMDA differentiation. (E) Graphs reporting quantification of percentage of DAT<sup>+</sup> over TH<sup>+</sup> neurons in these cultures at d50 of VMDA differentiation. Note a ~4-fold increase of DAT<sup>+</sup> neurons in the TH<sup>+</sup> population in GPC4sh vs CTRLsh cultures (CTRLsh:  $0.65 \pm 0.03\%$ ; GPC4sh:  $3.0 \pm 0.3\%$ ). Square and triangle symbols in graphs correspond to values calculated for GPC4sh5-c10 and GPC4sh4-c8 cells, respectively. Data are presented as mean  $\pm$  SEM (n = 2 biological replicates). Unpaired t test with Welch's corrections: \*P < .05. F and G, Immunostaining analysis showing the co-expression of (F) TH (green) with GIRK2 (red) or DAPI (blue) and (G) TH (green), CALBINDIN (red) or DAPI (blue), in CTRLsh, GPC4sh5-c10 and GPC4sh4-c8 cultures at d50 of VMDA differentiation. White arrowheads point at double positive neurons. Dashed squares in (G) indicate the position of the enlargement shown at their right side. Note the few CALBINDIN<sup>+</sup> neurons identified in CTRLsh and GPC4sh5-c10 cultures

Consistent with our previous *in vitro* analyses, immunohistochemical analyses showed no visible staining for OCT4 in the grafts suggesting lack of contaminating undifferentiated cells (data not shown). Similarly, we did not find expression of mesoderm (BRAC, TBX3; data not shown) and endoderm makers (SOX17; data not shown). Instead, we observed a broad staining for hNCAM (human-specific neural cell adhesion molecule) in CTRLsh and GPC4sh grafts showing the presence of a high proportion of human neural cells (Figure 6B). Furthermore, both grafts were enriched in NESTIN+ cells, indicating that cells were still at early stage of neural progenitor differentiation (Figure 6D). This was supported by the presence of SOX2 neural progenitors (Figure 6E) and of sporadic TH+ and MAP2+ cells

(Figure S8A and data not shown). Interestingly, we found a consistent presence of GFAP+ cells in both CTRLsh and GPC4sh grafts, with a slight increase of GFAP+ cells in GPC4sh grafts (Figure 6D). Of note, GFAP is a marker of astrocytes that, beyond their important roles in structural, metabolic support and synaptic transmission repair, are able to enhance DA neuron differentiation.<sup>39</sup>

We next studied the differentiation potential of the transplanted 5-days patterned VMDA cells by examining the distribution of progenitor markers by means of FOXA2 and LMX1A co-staining. Grafts from CTRLsh cells were enriched in FOXA2+ cells and displayed very sporadic LMX1A+ cells (Figure 7A,C), whereas GPC4sh-derived grafts were enriched in both FOXA2+ and LMX1A+

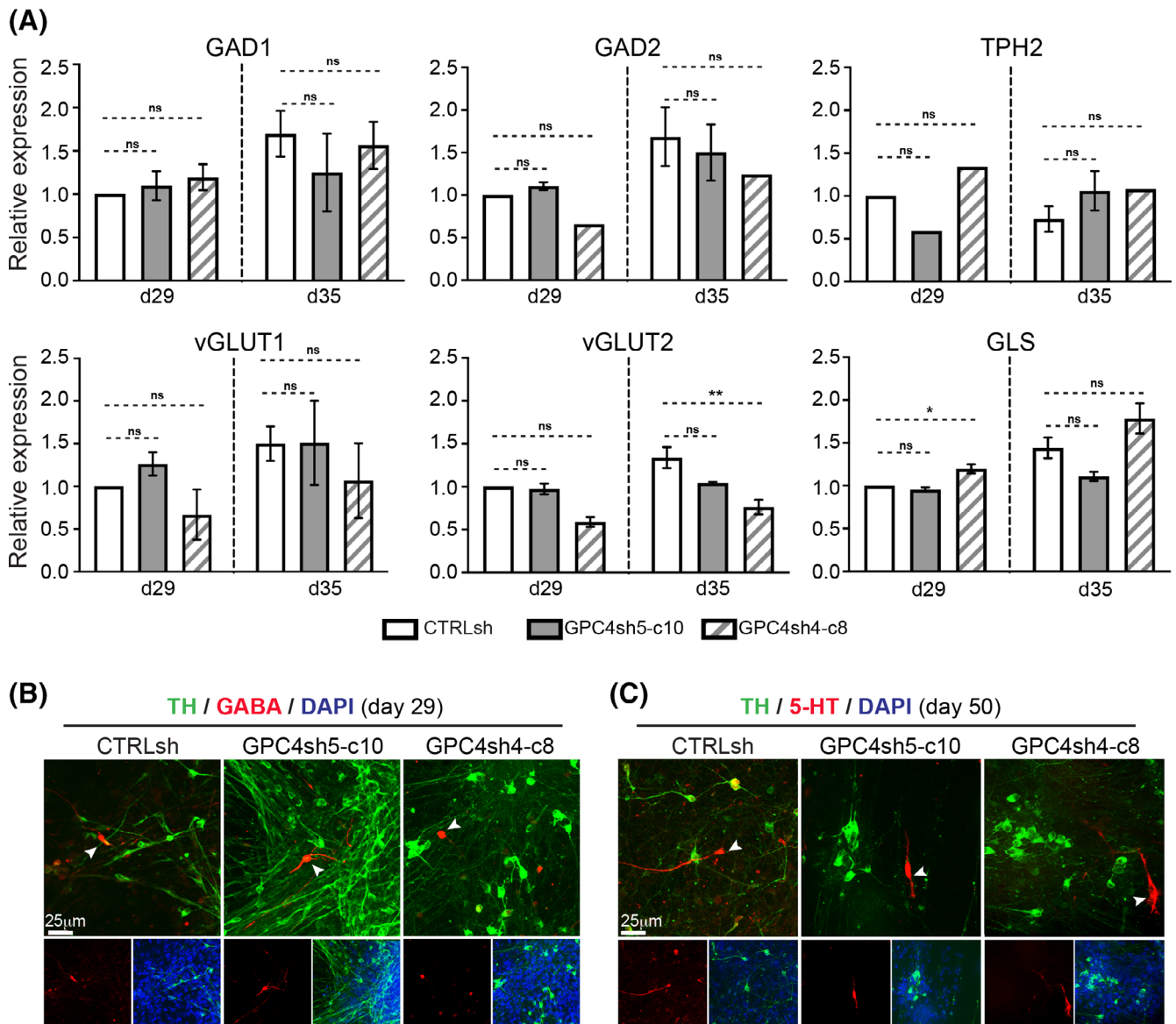


**FIGURE 5** GPC4 downregulation in hiPSCs does not increase the presence of GABAergic, serotonergic and glutamatergic neurons. A, Graphs reporting qRT-PCR analysis of GABAergic neuron markers (GAD1 and GAD2), serotonergic neuron marker (TPH2), and the glutamatergic neuron markers (vGLut1, vGLut2 and GLS) at d29 and d35 of *in vitro* VMDA neuron differentiation in CTRLsh, GPC4sh5-c10 and GPC4sh4-c8 cultures. Data are presented as mean  $\pm$  SEM ( $n = 2-3$  biological replicates). One-way ANOVA: ns = not significant. \* $P < .05$  and \*\* $P < .01$ . B and C, Immunofluorescence analyses of TH+ (green) and GABA+ (red) neurons (B) and of TH+ (green) and 5-HT+ (red) neurons (C) in cultures of the same lines at d29 of VMDA neuron differentiation. DAPI is in blue. White arrowheads point at the few identified GABAergic and serotonergic neurons

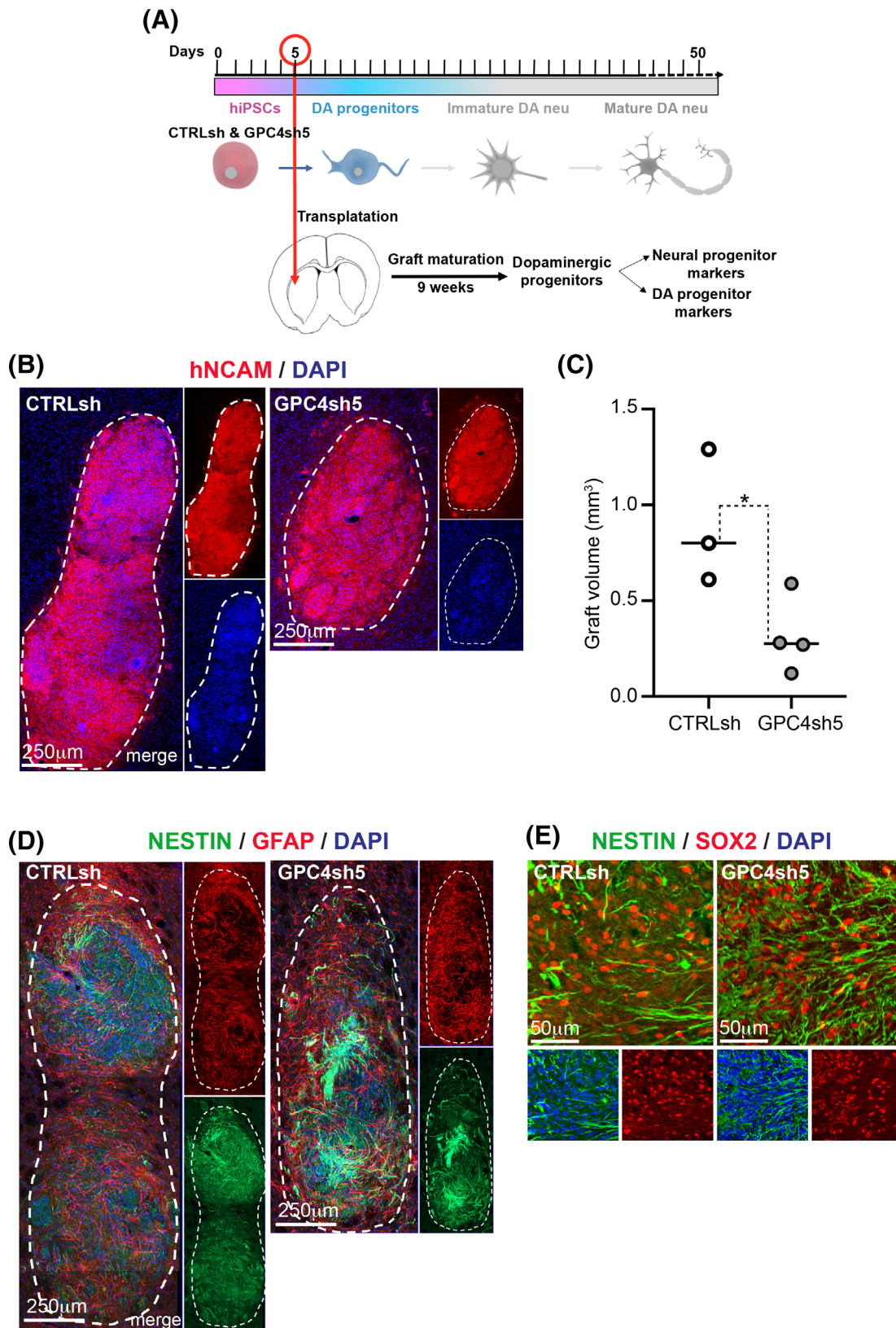


**FIGURE 6** Analysis of cell identity in brain grafts at 9 weeks post-transplantation. A, Schematic representation of the cell transplantation experiment with CTRLsh and GPC4sh hiPSC-derivatives. Forty thousand cells were grafted into the denervated striatum of adult rats with prior 6-hydroxydopamine-induced lesion of the nigrostriatal DA neurons. B, Overview of two representative grafts derived from transplantation of CTRLsh and GPC4sh5 hiPSC-derivatives after 9 weeks. Transplanted cells are visualized by the human specific NCAM marker. A white dashed line highlights the grafted area. C, Quantitative measurement of graft volume. Note that transplanted GPC4sh cells develop significantly smaller grafts. Data are presented as mean  $\pm$  SEM ( $n = 3$  for CTRLsh and  $n = 4$  for GPC4sh grafts). Unpaired  $t$  test:  $*P < .05$ . D and E, Immunohistochemistry of NESTIN (green), GFAP (red) and DAPI (blue) (D), and NESTIN (green), SOX2 (red) and DAPI (blue) (E) of grafts derived from transplantation of CTRLsh and GPC4sh5 cells. See also Figure S8

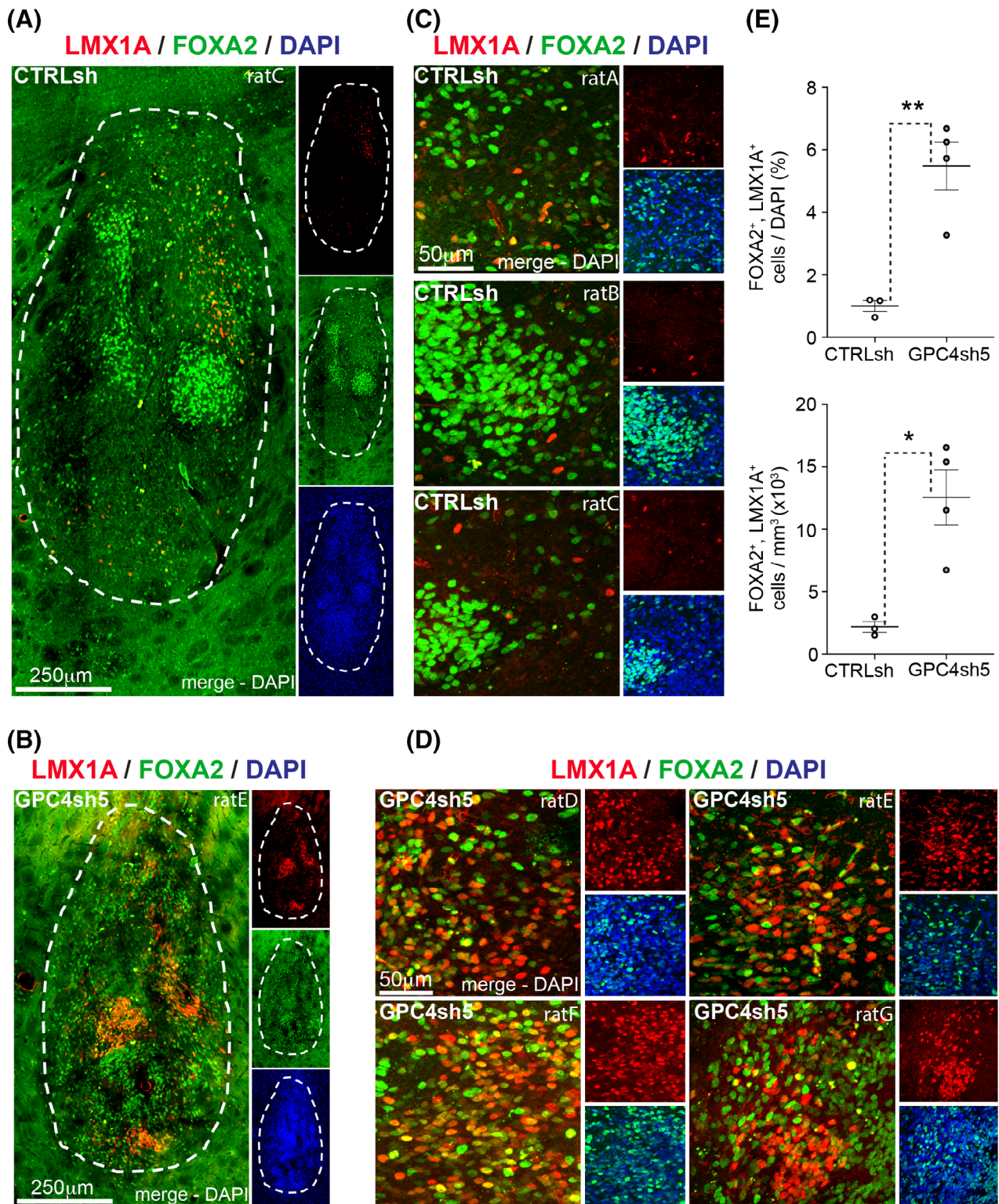


**FIGURE 7** Downregulation of GPC4 in hiPSCs promotes generation of VMDA progenitors after transplantation in rat brains. A and B, Overview of fluorescence immunostaining of FOXA2 (green), LMX1A (red), and DAPI (blue) in a rat brain section of striatal grafts originated from transplantation of CTRLsh (A) and GPC4sh cells (B) cells at d5 in vitro of VMDA neuron differentiation. The graft area is highlighted with a white dashed line. C and D, Distribution of FOXA2<sup>+</sup>, LMX1A<sup>+</sup> VMDA progenitors in three rats injected with CTRLsh (C) and in four rats injected with GPC4sh (D) cells. E, Graphs reporting the quantification of the percentage of double FOXA2<sup>+</sup> and LMX1A<sup>+</sup> over DAPI<sup>+</sup> cells (top panel) and over graft volume (bottom panel) in CTRLsh and GPC4sh5 grafts. Values for top panel are: CTRLsh:  $1 \pm 0.2\%$ ; GPC4sh:  $5.5 \pm 0.8\%$ . Values for bottom panel are: CTRLsh:  $2184 \pm 430/\text{mm}^3$ ; GPC4sh:  $12\,555 \pm 2217/\text{mm}^3$ . N = 3 for CTRLsh and n = 4 for GPC4sh grafts. Data are presented as mean  $\pm$  SEM (n = 3 for CTRLsh; n = 4 for GPC4sh grafts). Each dot represents an animal. Unpaired t test: ns = not significant, \*P < .05, \*\*P < .01

cells (compare Figure 7A with 7B and 7C with 7D). Quantitative analysis evidenced a  $\sim 2$ -fold increase of FOXA2+ (CTRLsh:  $14.5 \pm 1.9\%$  of DAPI+ cells; GPC4sh:  $27.7 \pm 8\%$ ), and a  $\sim 5$ -fold increase of LMX1A+ (CTRLsh:  $2.4 \pm 0.3\%$ ; GPC4sh:  $10.9 \pm 1.8\%$ ) in GPC4sh compared with CTRLsh grafts (Figure S8B). Finally, a  $\sim 5$ -fold increase was also found in the percentage of FOXA+/LMX1A+ double positive cells in GPC4sh grafts compared with CTRLsh cells (CTRLsh:  $1 \pm 0.2\%$ ; GPC4sh:  $5.5 \pm 0.8\%$ , Figure 7E). Expressing values as numbers of FOXA2+/LMX1A+ double cells vs graft volume confirmed these results (Figures 7E and S8C).

Taken together, these results show that hiPSCs transplanted after 5-days of in vitro VMDA differentiation into the striatum pursue efficiently toward the stage of VMDA progenitors at 9 weeks postgrafting. Moreover, they highlight the capability of transplanted GPC4sh hiPSC-derivatives to generate VMDA progenitors in a more efficient fashion than controls, thus indicating that downregulation of GPC4 in hiPSCs may be a strategy to enhance differentiation of hiPSCs in VMDA neurons also in vivo.

## 4 | DISCUSSION

A current challenge for the development of hiPSC-based disease modeling and cell replacement therapy for PD is to achieve efficient differentiation of suitable cell types from hiPSCs. In these studies, we identified the membrane bound HSPG, GPC4, as a key protein enabling manipulation of hiPSC fate. In particular, our loss-of function studies show that reducing GPC4 expression in hiPSCs significantly enhances their differentiation properties toward the VMDA neuron lineage both in vitro and upon brain transplantation without affecting hiPSC maintenance and stemness. Importantly, VMDA neurons derived from hiPSC with reduced GPC4 protein levels meet molecular criteria characterizing the SN VMDA neurons and complete the in vitro differentiation program by expressing proteins for DA synthesis, release and uptake. By characterizing the process of VMDA neuron differentiation, we discovered that the enhanced differentiation properties of hiPSCs with downregulated GPC4 relies on their increased capability to enter into the VMDA lineage and acquire a VMDA neural progenitor fate. Interestingly, such propensity is retained in vivo as GPC4sh cells grafted in the striatum of rat brains at floor-plate stage generate a 5-fold higher proportion of VMDA progenitors compared with controls. Thus, readjustment of the GPC4 protein levels allows the overall process of VMDA neuron differentiation from hiPSCs to become more efficient.

Mechanistically, GPC4 functions as cell membrane sensor of the extracellular environment and can interact with several signaling pathways, among which are the VMDA progenitor fate determinants, SHH, WNT and FGF.<sup>20,40</sup> At the cell membrane, GPC4 fine-tunes the cell perception of these signals by impacting on mechanisms such as receptor-ligand interactions, temporal and quantitative supply of active signals. These GPC4 functions are crucial for developmental processes, such as gastrulation and dorsal forebrain patterning in which GPC4 regulates WNT11 and FGF signaling activities, respectively.<sup>41,42</sup> As we have previously shown, these GPC4 functions also impact aspects of SC biology

as GPC4 positively modulate WNT/ $\beta$ -catenin signaling in self-renewing mESCs.<sup>24</sup> Control of FGF signaling by GPC4 levels might also operate at VMDA progenitor fate determination. Recent studies using mESCs and hESCs have reported that blockade of FGF signaling on exit of the lineage-primed epiblast pluripotent state initiates an early induction of LMX1A and FOXA2 in nascent neural progenitors. In addition to inducing VM characteristics, the FGF signaling blockade during neural induction directs midbrain fate by suppressing forebrain or caudal fates in embryos,<sup>18</sup> as we observed here in differentiating hiPSCs with downregulated GPC4. On the same line, addition of FGF8 to the differentiation medium of hESCs during the early phase of neural induction causes a reduced yield of VMDA progenitors.<sup>16</sup> Our expression analysis of GPC4 transcripts during VMDA neuron differentiation is compatible with a need for reduced GPC4 function during neural induction and acquisition of a VMDA progenitor fate. Thus, reducing GPC4 protein levels might contribute to establish the cell-signaling threshold underlying efficient VMDA neuron lineage specification. The higher proportion of VMDA progenitors in differentiating GPC4sh hiPSC cultures correlates with an increased number of differentiating cells expressing LMX1A. Previous studies have shown that forcing expression of LMX1A in hPSCs is sufficient to direct the fate of differentiating neural progenitors toward VMDA neurons of the SN subtype.<sup>43</sup> Moreover, a stepwise control of FGF and WNT signaling initiates an early induction of LMX1A in nascent neural progenitors.<sup>18</sup> These findings open the intriguing possibility that the molecular setting established in hiPSCs following GPC4 downregulation may confer a higher competence for LMX1A expression. Additional studies are needed to decipher the mechanism underlying the enhanced differentiation of hiPSCs toward VMDA progenitor fate following GPC4 downregulation.

Our in vivo studies also showed how robust can be the new molecular setting acquired by hiPSCs with downregulated GPC4. When transplanted in brains, GPC4 mutant neuroectodermal cells received only a short SHH and WNT treatment (5 days without FGF) and they were grafted upon acquiring a floor-plate stage. Despite these extreme conditions, transplanted cells engraft in the host striatum and become VMDA progenitors. It is still unclear whether the denervated striatum is a permissive environment for VMDA neuron differentiation and whether it releases survival or differentiation factors. Of note, our qRT-PCR data on cultured hiPSCs revealed endogenous expression of *SHH*, *WNT1*, and *FGF8* during VMDA neuron patterning in vitro. Therefore, one could hypothesize that these endogenously produced factors would continue to trigger VMDA neuron generation in vivo, and that downregulation of GPC4 in these cells would ensure their qualitative and quantitative actions.

Despite these unique differentiation features, downregulation of GPC4 in hiPSCs results in a new cellular system also displaying additional advantages at the undifferentiated stage. First, reduction of GPC4 does not affect other hiPSC biological properties such as undifferentiated growth characteristics, self-renewing ability, expression of stemness-associated transcription factors, and in vitro pluripotent differentiation potential, thus enabling a long-term maintenance of GPC4sh hiPSC lines. A second major advantage of hiPSCs with reduced GPC4 levels is their impaired potential for tumor development.

Tumorigenesis is a major risk for hiPSC-based regenerative therapy.<sup>44,45</sup> Cell transplantation studies into immunodeficient hosts have indicated that a threshold of undifferentiated cells ranging from 100 to 245 may be sufficient for tumor development.<sup>46,47</sup> To overcome tumor side risk, either postmitotic VMDA neurons or FACS sorted progenitors are currently desired for transplantation in PD patients.<sup>45</sup> Our data suggest that the approach of GPC4 downregulation in hiPSCs is relevant not only to enhance the differentiation of these cells toward VMDA lineage, but also to minimize the tumor side risk. As GPC4 is a cell surface protein, it may become an attractive “drugable” target to design strategies that may enable reaching the unique cell biological properties of GPC4sh hiPSCs without involving genetic manipulation.

## 5 | CONCLUSION

In conclusion, our study uncovers a new systematic approach that should enable the generation of hPSC lines most suitable for future translational applications. Our discoveries also present a novel entry point to define a new molecular mechanism underlying development of VMDA neurons of the SN subtype.

### ACKNOWLEDGMENTS

We thank: all members of our labs for helpful discussions and comments; A. Fico for critical reading of the manuscript; F. Shi and M. Sorce for contribution during the initial analysis of GPC4sh hiPSCs, and during the initial analysis of cell transplanted rat brain, respectively; A. Gagna for helping us to develop a mathematical method to calculate differentiation efficiency of different experiments; S. Lev and L. Khera for producing lentivirus particles carrying shRNA and for advises on use of lentivirus. Microscopy was performed at the imaging platform of the IBDM, supported by the ANR through the “Investments for the Future” program (France-BioImaging, ANR-10-INSB-04-01). The authors thank members of the IBDM core facility for microscopy and mouse husbandry for their technical support. This project is a part of the research program of the Centre of Excellence DHUNE, which is supported by the French National Plan on Neurodegenerative Diseases funded by the French Ministry of national education, higher education and research and the “Investissements d’Avenir” French Government program. The IBDM is affiliated with NeuroMarseille (AMX-19-IET-004), the AMU neuroscience network, and with NeuroSchool, the AMU graduate school in neuroscience supported by the A\*MIDEX foundation and the “Investissements d’Avenir” program (nEURO\*AMU, ANR-17-EURE-0029 grant). This work was funded by Association France Parkinson (Convention 096038), Fondation de France (2013\_00043173), SATT Sud-Est “Technology Transfer accelerator”, Programme de pré-maturation du Centre National de la Recherche Scientifique to R.D., Network of Centres of Excellence in Neurodegeneration (COEN Pathfinder III 4014) to R.D. and L.K.L.G., and was supported by Centre National de la Recherche Scientifique and Aix-Marseille Université. F.M. received support from FRM (Fondation Recherche Médicale; DEQ20141231766). S.C. was

supported by the BIOTRAIL PH.D. Program in Life Science, Marseille, France and by Association France Parkinson 4th year PH.D. fellowships. R.B. was supported by a grant from the Programme de pré-maturation du Centre National de la Recherche Scientifique to R.D. T.L. and D.R. were supported by the French Ministry of Higher Education, Innovation and Research fellowship. M.K. and E.A.T. were supported by the National Institute of Arthritis and Musculoskeletal and Skin Diseases; R01 AR075413. The funders had no role in study design, data collection and analysis, decision to publish, or preparation of the manuscript.

### CONFLICT OF INTEREST

The authors declared no potential conflicts of interest.

### AUTHOR CONTRIBUTIONS

S.C.: conception and design, methodology, collection and assembly of data, data analysis and interpretation, manuscript review and editing; R.B.: collection and assembly of data, manuscript proofreading; T.L., D.R.: collection and assembly of data, contribution to data analysis and interpretation, manuscript review and editing; C.M., P.S.: conception and design rat transplantation experiments, methodology rat transplantation experiments, visualization and interpretation rat transplantation experiment, manuscript visualization; E.A.T.: resources, methodology, manuscript visualization; M.K.: resources, methodology, manuscript review and editing, financial support; L.K.L.G.: conception and design rat transplantation experiments, manuscript review and editing, financial support; F.M.: contribution to design, manuscript review and editing, financial support; R.D.: conception and design, collection and assembly of data, data analysis and interpretation, financial support, manuscript original draft, review and editing.

### DATA AVAILABILITY STATEMENT

The single-cell RNA-seq dataset from human embryo VM cells used to analyze the expression of GPC1-6 has been published as additional data of the article: La Manno, G., Gyllborg, D., Codeluppi, S., Nishimura, K., Salto, C., Zeisel, A., Borm, L. E., Stott, S. R. W., Toledo, E. M., Villaescusa, J. C., et al. (2016). Molecular Diversity of Midbrain Development in Mouse, Human, and Stem Cells. *Cell* 167, 566-580 e519. <https://doi.org/10.1016/j.cell.2016.09.027>. Link: <http://linnarssonlab.org/ventralmidbrain/>. The expression profile of GPC4 in undifferentiated hESCs and hiPSCs was obtained from the StemMapper database published with the article: Pinto, J. P., Machado, R. S. R., Magno, R., Oliveira, D. V., Machado, S., Andrade, R. P., Braganca, J., Duarte, I. and Futschik, M. E. (2018). StemMapper: a curated gene expression database for stem cell lineage analysis. *Nucleic Acids Res* 46, D788-D793. <https://doi.org/10.1093/nar/gkx921>. Link: <http://stemmapper.sysbiolab.eu>.

### ORCID

Flavio Maina  <https://orcid.org/0000-0001-6100-4695>

Rosanna Dono  <https://orcid.org/0000-0002-7200-9464>

### REFERENCES

1. Kalia LV, Lang AE. Parkinson's disease. *Lancet*. 2015;386(9996):896-912.

2. Roeper J. Dissecting the diversity of midbrain dopamine neurons. *Trends Neurosci.* 2013;36(6):336-342.
3. Bjorklund A, Dunnett SB. Dopamine neuron systems in the brain: an update. *Trends Neurosci.* 2007;30(5):194-202.
4. Matsuda W, Furuta T, Nakamura KC, et al. Single nigrostriatal dopaminergic neurons form widely spread and highly dense axonal arborizations in the neostriatum. *J Neurosci.* 2009;29(2):444-453.
5. Blesa J, Przedborski S. Parkinson's disease: animal models and dopaminergic cell vulnerability. *Front Neuroanat.* 2014;8:155.
6. Pacelli C, Giguere N, Bourque MJ, et al. Elevated mitochondrial bioenergetics and axonal arborization size are key contributors to the vulnerability of dopamine neurons. *Curr Biol.* 2015;25(18):2349-2360.
7. La Manno G, Gyllborg D, Codeluppi S, et al. Molecular diversity of midbrain development in mouse, human, and stem cells. *Cell.* 2016;167(2):566-580.e519.
8. Hartfield EM, Yamasaki-Mann M, Ribeiro Fernandes HJ, et al. Physiological characterisation of human iPSC-derived dopaminergic neurons. *PLoS One.* 2014;9(2):e87388.
9. Yamanaka S. Induced pluripotent stem cells: past, present, and future. *Cell Stem Cell.* 2012;10(6):678-684.[in English].
10. Marrone L, Bus C, Schondorf D, et al. Generation of iPSCs carrying a common LRRK2 risk allele for in vitro modeling of idiopathic Parkinson's disease. *PLoS One.* 2018;13(3):e0192497.
11. Li H, Jiang H, Zhang B, Feng J. Modeling Parkinson's disease using patient-specific induced pluripotent stem cells. *J Parkinsons Dis.* 2018;8(4):479-493.
12. Kirkeby A, Nelander J, Parmar M. Generating regionalized neuronal cells from pluripotency, a step-by-step protocol. *Front Cell Neurosci.* 2012;6:64 [in English].
13. Kriks S, Shim JW, Piao J, et al. Dopamine neurons derived from human ES cells efficiently engraft in animal models of Parkinson's disease [research support, N.I.H., extramural research support, non-U.S. Gov't]. *Nature.* 2011;480(7378):547-551.[in English].
14. Stoddard-Bennett T, Pera RR. Stem cell therapy for Parkinson's disease: safety and modeling. *Neural Regen Res.* 2020;15(1):36-40.
15. Parmar M, Grealish S, Henschcliffe C. The future of stem cell therapies for Parkinson disease. *Nat Rev Neurosci.* 2020;21(2):103-115.
16. Kirkeby A, Nolbrant S, Tiklova K, et al. Predictive markers guide differentiation to improve graft outcome in clinical translation of hESC-based therapy for Parkinson's disease. *Cell Stem Cell.* 2017;20(1):135-148.
17. Nouri N, Patel MJ, Joksimovic M, et al. Excessive Wnt/beta-catenin signaling promotes midbrain floor plate neurogenesis, but results in vacillating dopamine progenitors. *Mol Cell Neurosci.* 2015;68:131-142.
18. Jaeger I, Arber C, Risner-Janiczek JR, et al. Temporally controlled modulation of FGF/ERK signaling directs midbrain dopaminergic neural progenitor fate in mouse and human pluripotent stem cells. *Development.* 2011;138(20):4363-4374.
19. Nolbrant S, Heuer A, Parmar M, Kirkeby A. Generation of high-purity human ventral midbrain dopaminergic progenitors for in vitro maturation and intracerebral transplantation. *Nat Protoc.* 2017;12(9):1962-1979.
20. Fico A, Maina F, Dono R. Fine-tuning of cell signaling by glypicans. *Cell Mol Life Sci.* 2011;68(6):923-929.[in English].
21. Fico A, Dono R. Signalling mechanisms underlying congenital malformation: the gatekeepers, glypicans. In: Sutcliffe A, ed. *Congenital Malformations.* United Kingdom: University College London, University of London; 2011.
22. Filmus J, Capurro M, Rast J. Glypicans. *Genome Biol.* 2008;9(5):224.
23. Yu C, Griffiths LR, Haupt LM. Exploiting heparan sulfate proteoglycans in human neurogenesis-controlling lineage specification and fate. *Front Integr Neurosci.* 2017;11:28.
24. Fico A, De Chevigny A, Egea J, et al. Modulating Glypican4 suppresses tumorigenicity of embryonic stem cells while preserving self-renewal and pluripotency [research support, non-U.S. Gov't]. *STEM CELLS.* 2012;30(9):1863-1874.[in English].
25. Fico A, de Chevigny A, Melon C, et al. Reducing glypican-4 in ES cells improves recovery in a rat model of Parkinson's disease by increasing the production of dopaminergic neurons and decreasing teratoma formation. *J Neurosci.* 2014;34(24):8318-8323.[in English].
26. Kim J, Magli A, Chan SSK, et al. Expansion and purification are critical for the therapeutic application of pluripotent stem cell-derived myogenic progenitors. *Stem Cell Rep.* 2017;9(1):12-22.
27. Schindelin J, Arganda-Carreras I, Frise E, et al. Fiji: an open-source platform for biological-image analysis. *Nat Methods.* 2012;9(7):676-682.
28. Pinto JP, Machado RSR, Magno R, et al. StemMapper: a curated gene expression database for stem cell lineage analysis. *Nucleic Acids Res.* 2018;46(D1):D788-D793.
29. Liu LP, Zheng YW. Predicting differentiation potential of human pluripotent stem cells: possibilities and challenges. *World J Stem Cells.* 2019;11(7):375-382.
30. Hebsgaard JB, Nelander J, Sabelstrom H, et al. Dopamine neuron precursors within the developing human mesencephalon show radial glial characteristics. *Glia.* 2009;57(15):1648-1658.
31. Barraud P, Thompson L, Kirik D, Bjorklund A, Parmar M. Isolation and characterization of neural precursor cells from the Sox1-GFP reporter mouse. *Eur J Neurosci.* 2005;22(7):1555-1569.
32. Smidt MP, van Hooft JA. Subset specification of central serotonergic neurons. *Front Cell Neurosci.* 2013;7:200.
33. Arenas E, Denham M, Villaescusa JC. How to make a midbrain dopaminergic neuron. *Development.* 2015;142(11):1918-1936.
34. Weihe E, Depboylu C, Schutz B, et al. Three types of tyrosine hydroxylase-positive CNS neurons distinguished by dopa decarboxylase and VMAT2 co-expression. *Cell Mol Neurobiol.* 2006;26(4-6):659-678.
35. Studer L. Derivation of dopaminergic neurons from pluripotent stem cells. *Prog Brain Res.* 2012;200:243-263.
36. Anderegg A, Poulin JF, Awatramani R. Molecular heterogeneity of midbrain dopaminergic neurons—moving toward single cell resolution. *FEBS Lett.* 2015;589(24 pt A):3714-3726.
37. Carta M, Carlsson T, Munoz A, et al. Role of serotonin neurons in the induction of levodopa- and graft-induced dyskinesias in Parkinson's disease. *Mov Disord.* 2010;25(suppl 1):S174-S179.
38. Qiu L, Liao MC, Chen AK, et al. Immature midbrain dopaminergic neurons derived from floor-plate method improve cell transplantation therapy efficacy for Parkinson's disease. *STEM CELLS TRANSLATIONAL MEDICINE.* 2017;6(9):1803-1814.
39. Yang F, Liu Y, Tu J, et al. Activated astrocytes enhance the dopaminergic differentiation of stem cells and promote brain repair through bFGF. *Nat Commun.* 2014;5:5627.
40. Desbordes SC, Sanson B. The glypican Dally-like is required for Hedgehog signalling in the embryonic epidermis of *Drosophila*. *Development.* 2003;130(25):6245-6255.
41. Ohkawara B, Yamamoto TS, Tada M, Ueno N. Role of glypican 4 in the regulation of convergent extension movements during gastrulation in *Xenopus laevis*. *Development.* 2003;130:2129-2138.
42. Galli A, Roue A, Zeller R, Dono R. Glypican 4 modulates FGF signaling and regulates dorsoventral forebrain patterning in *Xenopus* embryos. *Development.* 2003;130(20):4919-4929.
43. Cai J, Donaldson A, Yang M, German MS, Enikolopov G, Iacovitti L. The role of Lmx1a in the differentiation of human embryonic stem cells into midbrain dopamine neurons in culture and after transplantation into a Parkinson's disease model. *STEM CELLS.* 2009;27(1):220-229.
44. Fan Y, Winanto NSY. Replacing what's lost: a new era of stem cell therapy for Parkinson's disease. *Transl Neurodegener.* 2020;9:2.
45. Zakrzewski W, Dobrzynski M, Szymonowicz M, et al. Stem cells: past, present, and future. *Stem Cell Res Ther.* 2019;10(1):68.
46. Gropp M, Shilo V, Vainer G, et al. Standardization of the teratoma assay for analysis of pluripotency of human ES cells and biosafety of their differentiated progeny [research support, non-U.S. Gov't]. *PLoS One.* 2012;7(9):e45532 [in English].



47. Hentze H, Soong PL, Wang ST, Phillips BW, Putti TC, Dunn NR. Teratoma formation by human embryonic stem cells: evaluation of essential parameters for future safety studies. *Stem Cell Res.* 2009;2(3):198-210. [in English].

#### SUPPORTING INFORMATION

Additional supporting information may be found online in the Supporting Information section at the end of this article.

**How to cite this article:** Corti S, Bonjean R, Legier T, et al. Enhanced differentiation of human induced pluripotent stem cells toward the midbrain dopaminergic neuron lineage through GLYPICAN-4 downregulation. *STEM CELLS Transl Med.* 2021;10:725–742. <https://doi.org/10.1002/sctm.20-0177>